

Smart Bracelet using Haptic System with Fuzzy Controller in Demining Quad-rotor Robots

Yekkehfallah Majid, Yuanli Cai, GuaoYang, Naebi Ahmad, Matinfar Morteza
School of Electronic and Information Engineering, Xi'an Jiaotong University, Xi'an 710049, China

Abstract—In this paper we present a novel method based on haptic system and fuzzy logic controller that utilized a useful device in order to assist robot's pilot in controlling a demining quad-rotor robot in urgent situation. Moreover, we propose a smart bracelet that utilizes haptic system with fuzzy logic controller to generate desired vibration to user's hand with respect to mine detector sensor and sonar sensor, which are mounted on robot. In this approach, we design two separated bracelets for two user hands: the first one is for warning to user from mine detector sensor and the other one is for warning related to obstacle avoidance. Finally, we applied a medicines pulse sensor in fuzzy logic controller to measure pilot's heartbeat to help pilot in hazardous situation that this sensor connected to smart right bracelet.

Keywords—Haptic system, Fuzzy Logic, deminnig robot, vibrotactile, magnetic field.

Copyright © 2016. Published by UNSYSdigital. All rights reserved.
doi: [10.21535/jias.v3i2.910](https://doi.org/10.21535/jias.v3i2.910)

I. INTRODUCTION

AERIAL robot or quad-rotor robots are usually applied in hazardous areas and controlled remotely, including rescue or for measurement in dangerous places or places that are impossible for human to physically present there. Remote mobile robots are often preferable in hazardous environment, since it is not possible for autonomous mobile robots to operate there. A well-known example is demining robots. Tasks of demining robot are detecting mine in the mind field and marking it with tools mounted on the robot (**Figure 1**), and rescue [1]-[3]. In addition, some situations are very difficult or very dangerous for human to be physically present at the location [2]. Currently, robots controlled by human operators with visual display (**Figure 2**) and auditory sense, and operators are limited in their interaction with the robot. Because of difficult situation and the low threshold for dealing on demining tasks, minimizing operator's error while taking care for high level of accuracy and speed is difficult also if operator cannot clearly hear or see data from mine detector sensor (MDS) on operator's GUI (Graphical User Interface) (**Figure 2**). For these reasons, we used vibrotactile feedback according to the level of MDS's output and pulse of heartbeat (**Figure 12**) to inform user's hand to decrease

reaction of robot when robot is near dangerous touch with environment or when robot detects mine.

Accordingly, we propose two bracelets (Section III.C) for pilot's hand because this system gives two different kinds of warning to pilot: one bracelet for right hand which inform user when robot near dangerous touch with environment such as height warning and obstacle warning [4], and another one when MDS senses mine in landmine.



Figure 1 Photograph of the demining robot

This approach presents a smart bracelet with heartbeat pulse sensor based on Fuzzy Logic System (FLS) with feedback generator method for demining robots in teleoperation quad-rotor demining robot. The approach utilizes the MDS output and position of arm to generates desired vibrotactile using FLS. FLS is the best option when we use inaccurate data as inputs and outputs such as shown in **Figure 7**. Application of demining robot in detecting mines in landmine without any touch by using MDS is discussed in Section II.B.

In this paper, we investigated problems of previous work on demining robot (**Figure 1**) such as safety controlling and operator's error. We added new sensor to use influence of user's heartbeat (Section III.D) on reaction of robot. In addition, we presented smart bracelet in order to decrease operator's faults and smart controller by defining force zone for dynamic parametric field (**Figure 16** & **Figure 19**) with respect to those parameters. In addition, we define our algorithms to send different warning to pilot: an FLS controls the rate of the vibrotactile to one hand, and to the other hand, another FLS controls the speed of the quad-rotor according to the heartbeat of the pilot the partition of this paper is in the following. In

Section II, we described previous work on demining robot; in Section III we explained our proposal in detail. In section I where we implemented FLS and haptic system in MATLAB fuzzy tools, while in Section V we concluded result of implementation in Section I.

II. BACKGROUND

A. Demining Wheeled Robot

United Nations reports show that every year, landmines kill more than 10,000 people, most of them are children. Scattered over area in nearly 78 countries [1], some of these mines were left from some years ago during wartime, and only some of them are detected. In recent years, mines have been used increasingly as weapons of terror against local civilian population village and roads. These are enough reasons to develop demining robot in all over the world.

Principally, mobile demining teleoperation robot for mine detection uses MDS mounted on the robot, and the user controls this robot by joystick. But it becomes difficult when it has to move in area with harsh terrain such as rocky mountainous land, and also it needs to pass through land mine physically. In Section III, we explain our proposal to solve the problems that we mentioned. In this system, interaction between user and robot only with one remote controller and with visual display, and there is no more feedback from robot to user.



Figure 2 Operator GUI that contains camera monitoring, robot controller, and a mine illustrate, network monitoring, robot's batteries status illustrates, and laptop's battery status illustrates, motors statuses indicators

This console was developed in windows, and this is a graphical console between operator and robot, this console installed in operator computer (Figure 8).

B. Mine Detector Sensor (MDS)

MDS works by transmitting a magnetic field and analyzing a return signal from the target and environment. These systems may use a single coil as both transmitter and receiver, or they

may have two or even three coils working together. In this project, we used two coils: first coil is signal transmitter and second one is signal receiver (Figure 3).

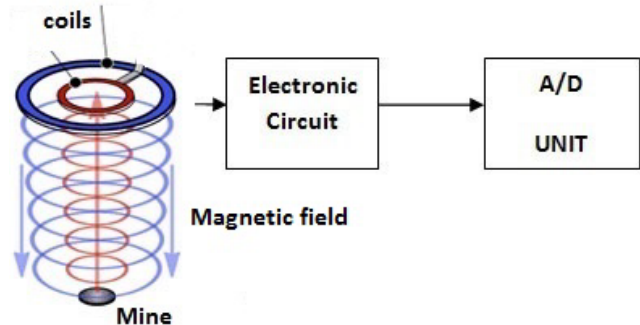


Figure 3 Overall hardware of mine detector sensor

Basically, Electronic section has two parts that one section belongs to the transmitter, and the second one is the receiver part which gets magnetic feedback and conveys it to the electronics, that in turn transfers analog signal of the output signal to A/D (analog to digital) block of microcontroller. Level of the output is related to two items that one is distance between mine and coil (Figure 7), and the second one is size of the mine.

A simple circular metal with 15 cm in diameter is used for testing of the MDS, and in Figure 7, level of the MDS's output is related to distance of the target, truly distance of the target with MDS has an inverse relationship.

C. Electromagnetic Induction

This section analyzes MDS part because, in fuzzy logic, we need to know about our input such as maximum distance that MDS can detects mine under the ground.

As we mentioned before, in this section there are two parts that first one is transmitter and second one is receiver, and we simulated this two coils with FEMM (Figure 4) [5] [6]. In Figure 4, MDS and a mine are drawn in the axis-symmetric solver by placing nodes and connecting them by lines. FEMM is one of power full software that uses for designing and analyzing magnetic problems [7] [8].

Transmitter coil generates electromagnetic field and according to mutual inductance effect which described by faraday's law of induction and Lenz's law [9], the induced EMF in receiver coil caused by the change in flux (Φ) can be expressed as:

$$\varepsilon = -N \frac{d\Phi}{dt} \quad (1)$$

where ε is the electromotive force (EMF), Φ is the magnetic flux, N is tightly wound coil of wire that composed of N identical turns and t is time [9].

When there is no mine near coil, the flux is constant (Figure 5); when there is a mine near coils, flux will change with respect

to distance of coils and a mine (Figure 6). Therefore, according to Equation (1) when flux changed, induced EMF in receiver coil will change. Meanwhile, electronic circuit that is connected to receiver will sense these variations and transfers it to A/D section, and this part delivers to fuzzy logic system.

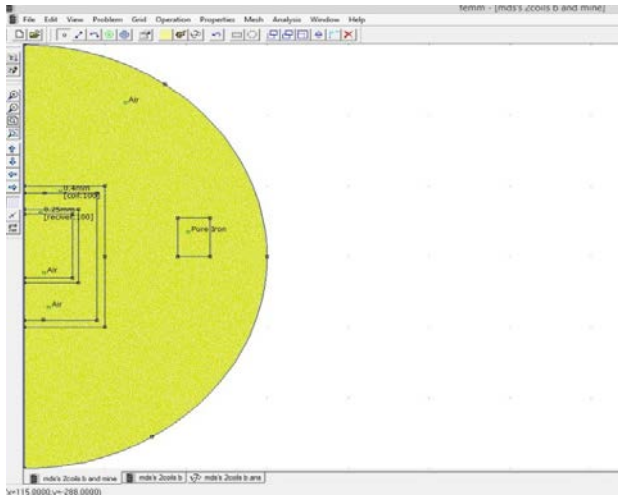


Figure 4 A screenshot of interface of FEMM, completed coils and mine model, ready to be analyzed. a) Transmitter coil b) receiver coil c) mine d) defined region for analyzed

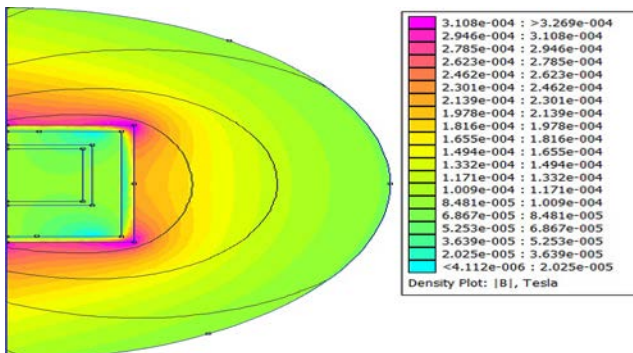


Figure 5 Color flux density plot of two coils without mine

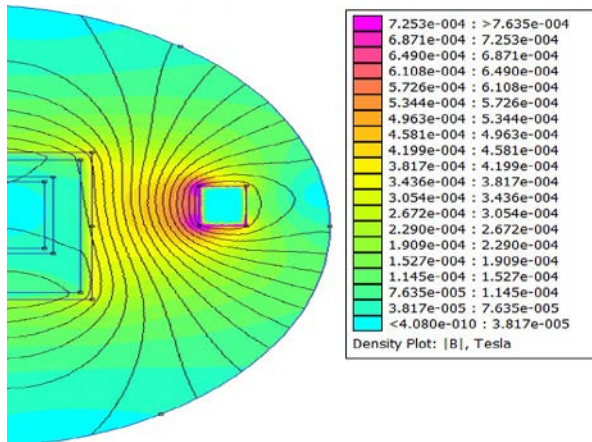


Figure 6 Color flux density plot of two coils with mine

In Figure 5 the transmitter coil generates magnetic flux and causes to generate EMF in the receiver coil according to Equation (1)., The influencing property of the space between the

two coils is just air reluctance (Equation (2)) and the flux is distributed equally in whole of analyzed region.

Figure 6 is the same as the plot in Figure 5, except that there is a mine in the analyzed region. Most of the flux passes through the mine because the reluctance of the mine is smaller than that of the air. Therefore, less flux passes through the receiver coil and induces less EMF in the receiver coil.

$$R = \frac{l}{A \times \mu_0 \times \mu_r} \quad (2)$$

where R is reluctance of a magnetic circuit, l is length of the circuit in meter, μ_0 is permeability of vacuum, μ_r is the relative magnetic permeability of the material, μ_0 permeability of the material, A is the cross-sectional area of the circuit in square meters [9].

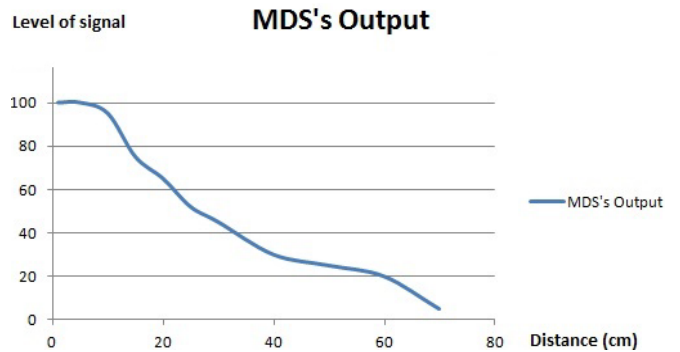


Figure 7 Level of MDS's output related to target distance

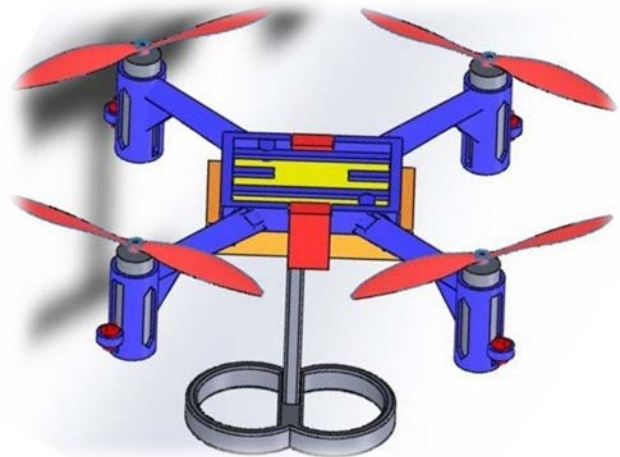


Figure 8 Quad-rotor robot with mine detector mounted on the bottom of robot

III. PROPOSED METHOD

A. Quad-rotor Robot

We propose a demining quad-rotor robot because this robot can go through air without any touch with landmine, allowing it to detect the mine safely and report it to pilot. Moreover, other advantages of quad-rotor in our proposal are low dimension, good maneuverability, simple control and payload capacity, in addition to being particular for demining tasks, for sampling in

dangerous environments, and for navigation in outdoor mapping. This robot is equipped with camera, sonar and IR (infrared sensor) sensor, IMU (Inertial Measurement Unit), ZigBee, MDS, barometer and mainboard (**Figure 14**).

For control quad-rotor we need to realize more about dynamic, kinematic and behavior of quad-rotor robot [10][11][12]. In this paper, we explain selected important equations of quad-rotor that have important roles in this proposal.

B. Dynamics and Kinematic of Quad-rotor

The inertial frame is defined by the ground, with gravity pointing in the negative z direction. The body frame is defined by the orientation of the quad-rotor, with the rotor axes pointing in the positive z direction and the arms pointing in the x and y directions. This work focuses on our controller and dynamic and kinematic of quad-rotor. Since our work's focus is on the controller, we only present a brief discussion about the dynamics and kinematics in this paper but we just mentioned on some important section of dynamic and kinematics of this robot.

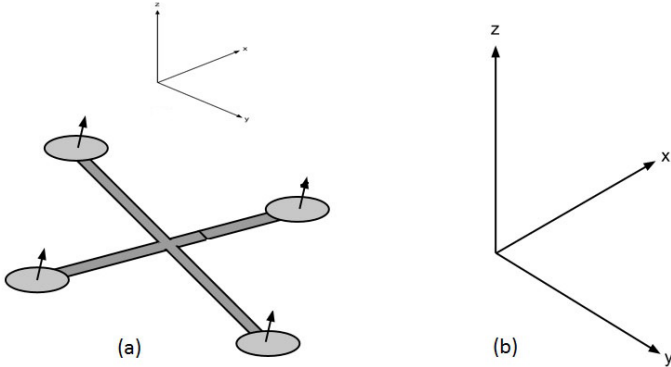


Figure 9 Body frame and inertial frame of quad-rotor robot

The rotation of a rigid body in space can be parameterized using several methods like Euler angles, Quaternions and Tait-Bryan angles [13].

$R(x, \phi)$ rotation around x-axis.

$R(y, \theta)$ rotation around y-axis.

$R(z, \Psi)$ rotation around z-axis.

Therefore, they are given by:

$$R(x, \phi) = \begin{pmatrix} 1 & 0 & 0 \\ 0 & \cos \phi & -\sin \phi \\ 0 & \sin \phi & \cos \phi \end{pmatrix} \quad (3)$$

$$R(y, \theta) = \begin{pmatrix} \cos \theta & 0 & \sin \theta \\ 0 & 1 & 0 \\ -\sin \theta & 0 & \cos \theta \end{pmatrix} \quad (4)$$

$$R(z, \psi) = \begin{pmatrix} \cos \psi & -\sin \psi & 0 \\ \sin \psi & \cos \psi & 0 \\ 0 & 0 & 1 \end{pmatrix} \quad (5)$$

The final rotation matrix is product of previous three relations:

$$R(\phi, \theta, \psi) = R(x, \phi)R(y, \theta)R(z, \psi) \quad (6)$$

Therefore:

$$R(\phi, \theta, \psi) = \begin{pmatrix} \cos \theta \cos \psi & \sin \theta \cos \psi \sin \phi - \sin \psi \cos \theta & \cos \psi \sin \theta \cos \phi + \sin \psi \cos \phi \\ \cos \theta \sin \psi & \sin \theta \sin \psi \sin \phi + \cos \psi \cos \theta & \sin \theta \sin \psi \cos \phi - \sin \phi \cos \psi \\ -\sin \theta & \cos \theta \sin \phi & \cos \theta \cos \phi \end{pmatrix} \quad (7)$$

C. Control Fundamentals

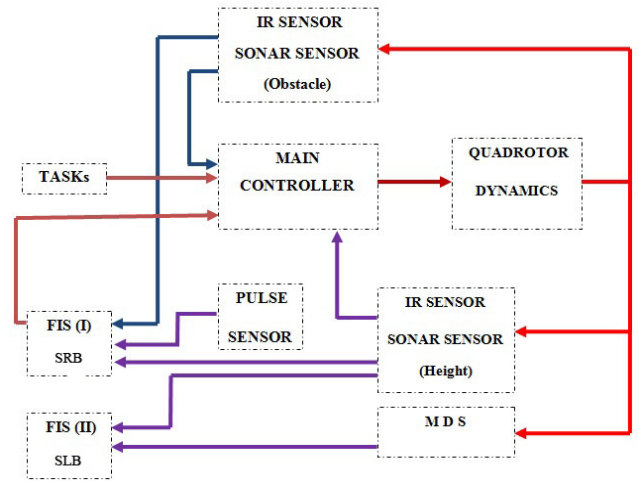


Figure 10 control block diagram of quad-rotor robot, SRB stands for Smart Right Bracelet, SLB for left one

In the block diagram in **Figure 10** is the control algorithm of the main control of the robot. Task of the main control is processes of quadrotor robot to control Euler angle and rotation of robot **Equation (3)**, **(4)**, and **(5)** and rotation **Equation (7)**. In addition, we added two fuzzy logic systems to control the value of the vibrotactile with respect to MDS, and we can control the speed of the quad-rotor base on pilot's heartbeat. One belongs to vibrotactile of right bracelet (**TABLE II**) which warns user when robot near dangerous touch with obstacle. The other output is related to pulse sensor (**TABLE II**); when rate of pilot's heartbeat goes up, this part sends command to main control to reduce speed of robot. FIS (II) belongs to left bracelet (**TABLE I**) that control the value of vibrotactile in SLR with respect to MDS and Z axis.

For more complex systems, a more continuous approach is necessary; there linear feedback control can be used. One of simplest implementation of linear feedback control is proportional control. In this sense, the control system actuates

the system in proportion to the current error between the actual operation point and desired set point.

In **Figure 11**, d is actual desired set point and O is output of system. d reference signal compared via negative feedback to the measured output from the sensor. This compression is the error signal (e), which is the input of the controller. The controller forces this error signal to zero through proportional, integral and derivation controls.

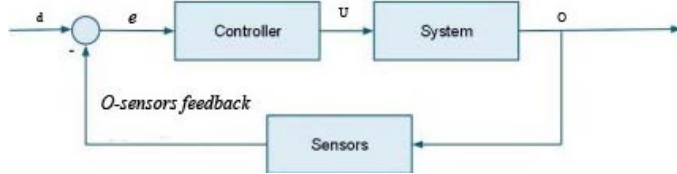


Figure 11 fundamental controller of algorithm controller

D. Smart Bracelets

As mentioned in Section II we had some problems in previous work such as noisy environment [1] and network delay for transferring video data to pilot, and GUI for operator is not effective in all situations. Pilot should care to obstacles in environment while checking MDS's indicator in GUI at the same time. For these reasons, we propose two smart bracelets that inform user using vibrotactile feedback. It means, whenever the robot gets into dangerous situation, the smart bracelets will convey vibration to user hands informing pilot about dangerous touch. Our approach uses haptic system with fuzzy logic controller. For haptic system, we used three electric motors in smart bracelet (**Figure 12**). Haptic increases human sensitivity from environment and pilot's hand can feel obstacle and the mine through vibrotactile feedback and in other hand this work utilizes pulse sensor to measure rate of pilot's heartbeat, with reference to rate of the heartbeat fuzzy logic reduces the reaction of the robot in dangerous situation.

In order to control speed of the motors, most of quad-rotor robots used brushless motors for four electric motors; the torque produced is given by:

$$\tau = k_p (I - I_0) \tag{8}$$

where τ is torque of motors, I is input current, I_0 is the current when there is no load on motors, and k_p is torque proportionality constant.

The voltage across the motor is given by:

$$V = IR_m + K_V \omega \tag{9}$$

where V is the voltage drop across the motor, R_m is the motor resistance, ω is the angular velocity of the motor, and K_V is a proportionality constant (indicating back-EMF generated per RPM). With respect to this equation we can control speed of the motor with control voltage of the motor.

E. Pulse Sensor

Pulse sensor is a well-known medical device used for non-invasive heart rate monitoring. It is also a low power device that it is great for low power and mobile applications.

By clipping a pulse sensor to the user's earlobe, it measures the pulse and transfers pulse data to the MCU in smart bracelet (**Figure 12**). This sensor helps us to have safe controller in urgent situation. When the pilot is in urgent situation, the rate of the pilot's pulse goes up [14]. This situation may be caused by the pilot's mistake. For such situation, we use pulse sensor's data in controller of quad-rotor to reduce the speed of robot with respect to pulse rate.

MDS unit detects the mine under the ground (**Figure 3**) and send data through ZigBee to the vibrotactile controller on left bracelet. After fuzzification, vibrotactile section sends vibration data to vibration motor part.

As mentioned above, there are three FLSs: one on the left bracelet that controls the level of vibrotactile, the other two on the right bracelet that control speed of the robots and vibrotactile controller (**Figure 11**). For implementation, we use MATLAB toolbox with MAMDANI method [15].

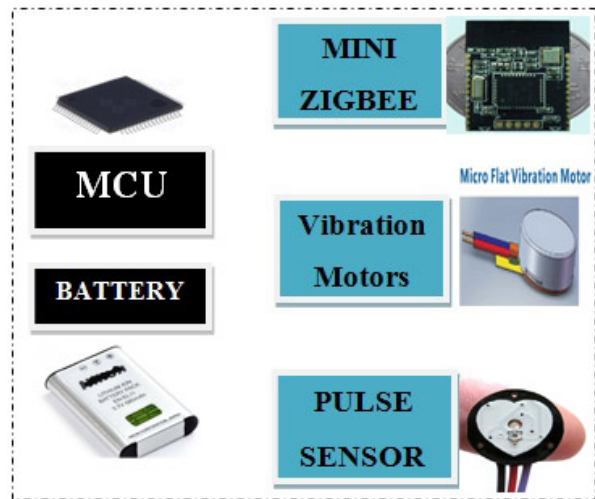


Figure 12 Overall framework of smart bracelet

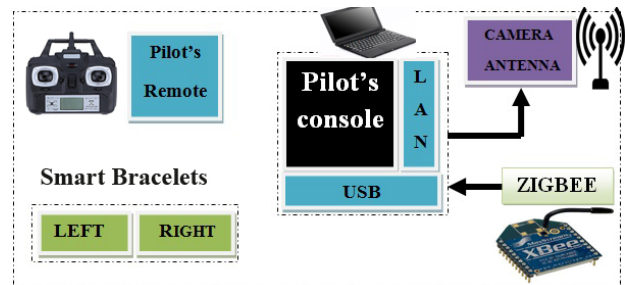


Figure 13 Pilot side in operator room

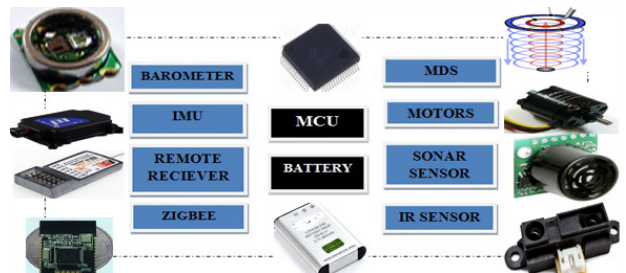


Figure 14 Overall framework of quad-rotor robot

IV. IMPLEMENTATION

Trap membership function used for MDS inputs and outputs in three FLSs are presented in **Figure 15** and **Figure 20**. The rule based in this work is shown in **TABLE I**, **TABLE II** and **TABLE III**, the commonly used Madman’s min-max implication function was utilized. Finally, for defuzzification we used centroid technique because it is very accurate. The control surface generated by the rule bases and the given fuzzy sets is depicted in **Figure 17**, and **Figure 21**. Detail of fuzzy logic system could be found in literature [16][17].

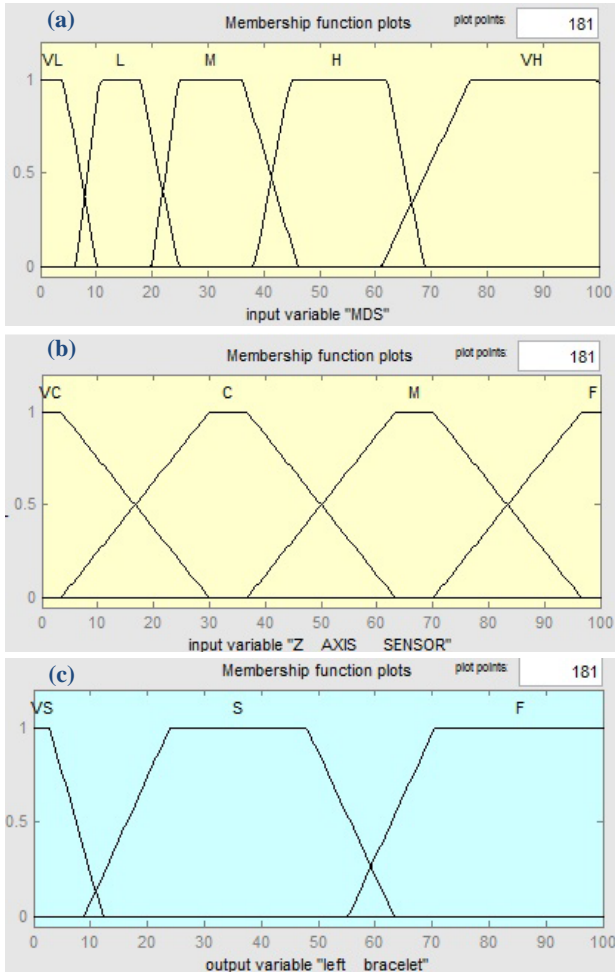


Figure 15 (a) Membership functions of MDS; (b) Membership function of z axis status; (c) Membership function of vibrotactile

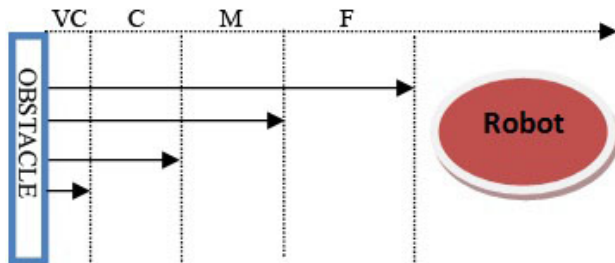


Figure 16 Force zone for dynamic parametric field

In **TABLE I** we divide MDS value to four parts and distance to ground in z axis (Z axis) to three parts as shown in table. When the MDS level increases, robot is very close to ground or obstacle.

Respectively, members of fuzzy function in **TABLE I** are decomposed into three fuzzy partitions for vibrotactile: very slow (VS), slow (S), Fast (F), and four partition for MDS: very low (VL), low (L) high (H) and very high (VH), in last portions related to Z-axis as: very close (VC), close (C), far (F).

Another important section in this research for us is altitude controller because robot needs have accurate controller for obstacle avoidance while searching.

Pressure-based altimeter constitutes a lightweight and economical way of measuring the altitude of a flying machine. Their precision can reach the order of decimeters making them more accurate than GPS receiver, especially when coupled with other sensors. The main disadvantage of barometric altimeter is that the air pressure tends to change slowly with the time due to meteorological effects. Its noise process is therefore time correlated. Obviously, the measured pressure is also affected by the local air turbulence (produced both by wind and the propellers). Following [11][13], we model the altimeter measurements as follows:

$$\begin{aligned}
 h &= -p_z + b_h + v_{hm} \\
 \dot{b} &= -\frac{1}{\tau_b} b + v_{hc}
 \end{aligned}
 \tag{10}$$

where h is altimeter output, $-p_z$ is the true altitude, b_h is the bias noise and v_{hm} is white Gauss-Markov process with time constant τ_b driven by the white Gaussian noise v_{hc} . It is worth noting that $-p_z$ is due to our choice of following the aeronautic convection and adopting a special body frame.

Due to uncertain data in real world (input in MDS and Z axis part), we don’t have exact region as force zone in **Figure 16** we estimated with fuzzy logic system as (**Figure 15a**) and (**Figure 15b**).

This three-dimensional plot illustrates two inputs as MDS and z axis sensor and output of this plot shows level of the vibrotactile in left bracelet.

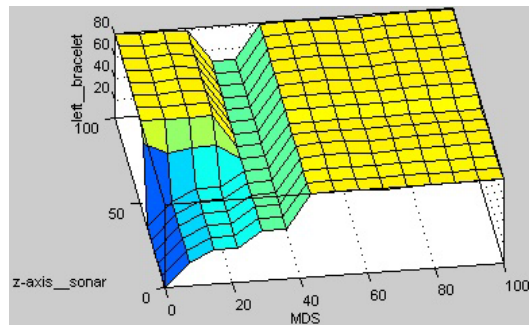


Figure 17 The output surface of the implemented fuzzy vibrotactile, generator for left bracelet

TABLE I RULE TABLE OF THE VIBROTACTILE CONTROLLER WITH RESPECT TO MDS OUTPUT AND Z-AXIS

MDS	Z AXIS	VC	C	F
	VL	VS	VS	F
	L	S	S	F
	H	F	F	F
	VH	F	F	F

TABLE II RULE TABLE OF THE VIBROTACTILE CONTROLLER WITH RESPECT TO Z-AXIS AND OBSTACLE SENSORS

Z AXIS	OBSTACLE SENSOR	VC	C	M	F
	VC	F	F	F	M
	C	F	F	M	M
	M	F	M	S	VS
	F	M	M	VS	VS

TABLE III RULE TABLE OF THE SPEED CONTROLLER WITH RESPECT TO PULSE SENSOR AND OBSTACLE SENSORS

PULSE SENSOR	OBSTACLE SENSOR	VC	VC	M	F
	N	N	N	N	N
	M	W	N	N	N
	F	D	D	W	W
	VF	D	D	W	N

A. Right Bracelet

In right bracelet has two parts. The first one belongs to the pulse sensor which measures heartbeat of the pilot and controls the speed of the robot according to **Equation (8)** and **Equation (9)**. The second one is related to the vibrotactile part which informs the pilot with vibration in urgent situations.

Implementation of this part is different with first FIS:

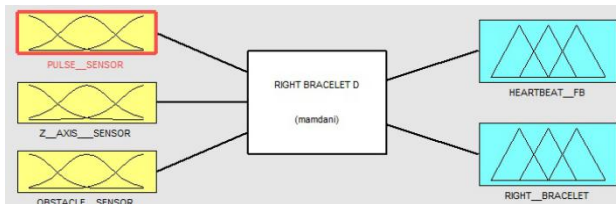


Figure 18 FIS (II) with three inputs and two outputs

Respectively, **TABLE II** contains four partitions for output: very slow (VS), Slow (S), moderate (M), fast (F). It also contains three partition for Z-axis as: very close (VC), close(C), moderate (M) and far (F). The last portions are related to sensors of obstacle which are the same as z axis part.

Respectively, **TABLE III** is the same as **TABLE I** and **TABLE II** that it contains three partitions for output: normal (N), warning (W), danger (D), and four partition for pulse sensor as: normal (DP), moderate (M), fast(F), very fast (VF). The last portion of obstacle sensor is explained in **TABLE III**.

Due to uncertain data we do not have exact region as in real world (**Figure 19**). We estimated these zones with fuzzy logic system as (**Figure 20a**) to (**Figure 20e**).

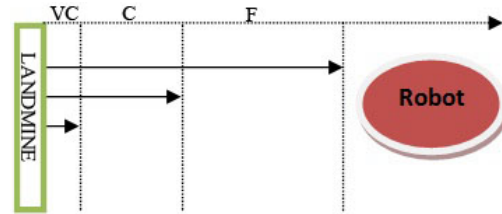


Figure 19 Force zone for dynamic parametric field

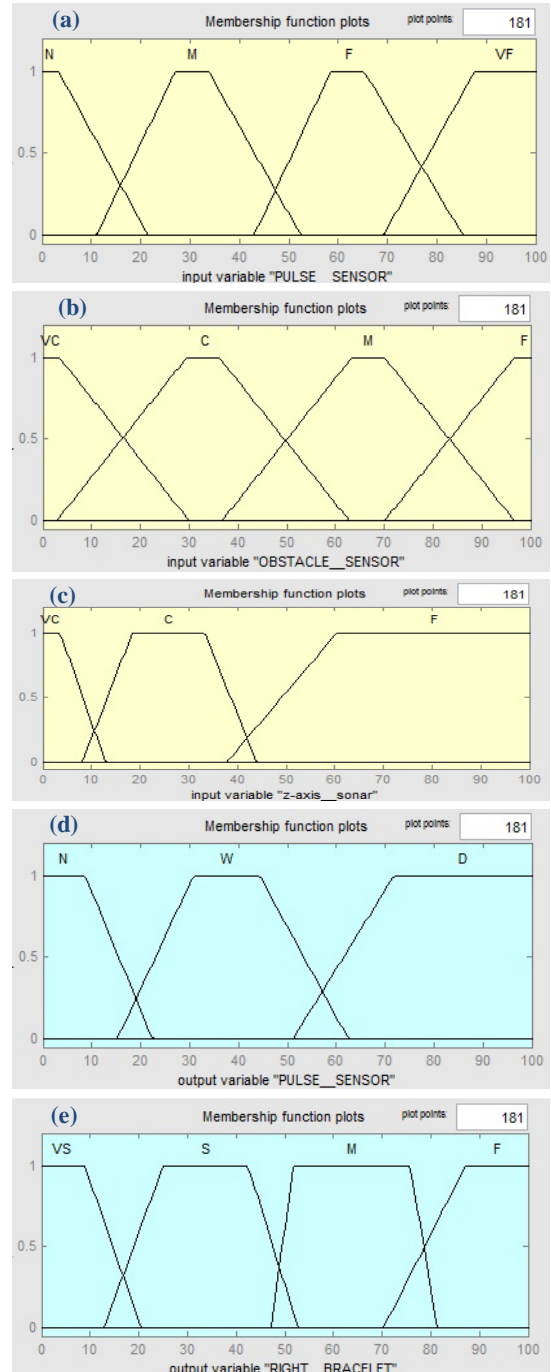


Figure 20 (a) Membership functions of pulse sensor; (b) Membership function of obstacle sensor; (c) Membership function of z axis; (d) Membership functions of output pulse sensor; (e) Membership functions of vibrotactile output for right bracelet

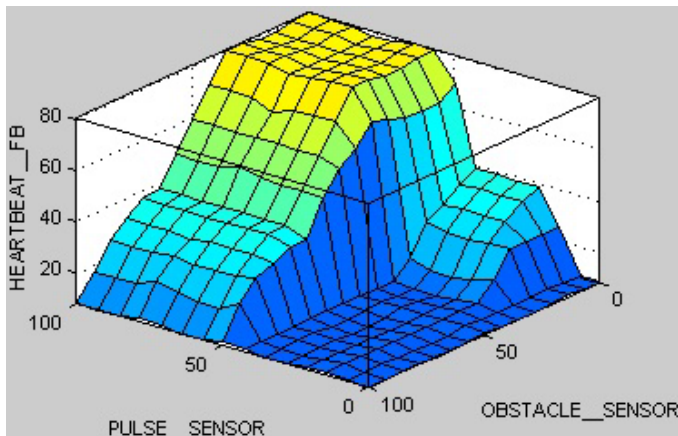


Figure 21 The output surface of the implemented fuzzy of heart beat feedback (speed controller)

A three-dimensional curve represents mapping function from pulse sensor and obstacle sensors; this curve represents a two-input and one output case.

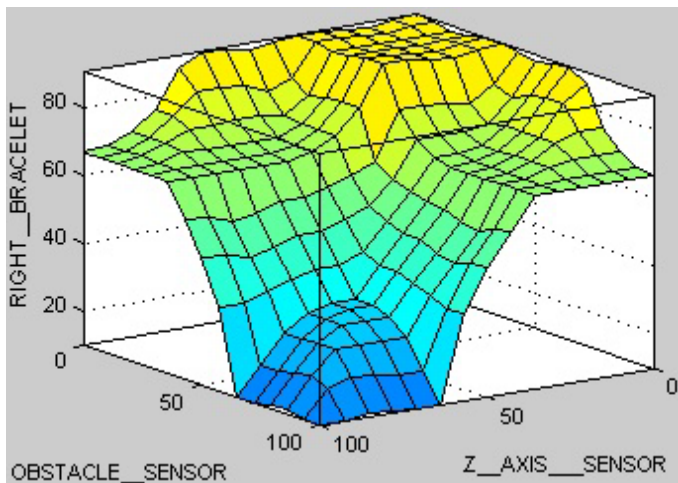


Figure 22 The output surface of the implemented fuzzy vibrotactile, generator

There are two inputs in this three-dimensional curve: input from z-axis sensor and that from obstacle sensor. The output of this curve is the level of the vibrotactile for right bracelet.

V. CONCLUSION

This paper presents two novel safety smart bracelets that utilize haptic system and fuzzy controller to warn the pilot of demining quad-rotor robot to avoid dangerous touch with obstacle. The bracelets also enhance the control speed of the robot using measurement on the pulse of the pilot.

In this method, we do not need to design new remote controller because we design two different modules as bracelet on pilot's hand that is separated from the remote controller.

This paper considers demining quad-rotor robot and simulating the force feedback effect for SLB and SRL on MATLAB fuzzy toolbox. In addition, this paper illustrates our result in three-dimensional curve with this toolbox. SLB informs the pilot from those errors which is related to MDS and Z-axis, while SRB convey vibrotactile feedback to pilot with two inputs as obstacle sensors and z-axis sensors. A pulse sensor is also connected to SRB in order to measure heartbeat rate and transfer it to the main control of the robot. The results show that with a smart bracelet in tele-operation demining robots, we can significantly reduce pilot's mistake during landmine searching operation, and make self-confidence to pilot during searching.

ACKNOWLEDGMENT

This work supported in part by the national natural science foundation of China (Grant No.61673314 and No.61573272), and the Xi'an Jiotong University and MRL laboratory of Qiau.

REFERENCES

- [1] SibertSibert, J., Cooper, J., Covington, C., Stefanovski, A., Thompson, D., and Lindeman, R.W. 2006. Vibrotactile feedback for enhanced control of urban search and rescue robots. In Proceedings of the IEEE Symposium on Safety, Security and Rescue Robots(Gaithersburg MD, August 22-24, 2006)
- [2] Yekkehfallah Majid, Yuanli Cai, Guao Yang, et al. "Haptic system with fuzzy controller for extended control of Teleoperation mine detector wheeled robots". The 2016 International Conference on Artificial Life and Robotics (ICAROB 2016), Jan. 29-31, Okinawa, Japan, pp.285-288.
- [3] Smith, F. M., D. K. Backman, and Stephen C. Jacobsen. "Telerobotic manipulator for hazardous environments." *Journal of Robotic Systems*, 1992,9(2): pp.251-260.
- [4] Brandt, A. M., & Colton, M. B. Haptic collision avoidance for a remotely operated quad-rotor uav in indoor environments. 2010 IEEE International Conference on Systems Man and Cybernetics (SMC), pp. 2724-2731.
- [5] Meeker, David. "FEMM 4.2 Electrostatics Tutorial1." (2006).
- [6] Jin, Jian-Ming. The finite element method in electromagnetics. John Wiley & Sons, 2014.
- [7] Turner, Robert. "Gradient coil design: a review of methods." *Magnetic Resonance Imaging*, 1993, 11(7): 903-920.
- [8] Singh, Isha, and Rajul Mishra. "Analysis of Magnetic Field of Air Cored Solenoid using FEMM."
- [9] Fitzpatrick, Richard. *Maxwell's Equations and the Principles of Electromagnetism*. Jones & Bartlett Publishers, 2008
- [10] Rodić, Aleksandar, and Gyula Mester. "The modeling and simulation of an autonomous quad-rotor microcopter in a virtual outdoor scenario." *Acta Polytechnica Hungarica*, 2011, 8(4): 107-122.
- [11] Liu, H., Li, D., Xi, J., and Zhong, Y. Robust attitude controller design for miniature quad-rotors. *Int. J. Robust. Nonlinear Control*, 2016, 26: 681-696. doi: 10.1002/rnc.3332.
- [12] Derafa, L., A. Benallegue, and L. Fridman. "Super twisting control algorithm for the attitude tracking of a four rotors UAV." *Journal of the Franklin Institute*. 2012, 349(2): 685-699.

- [13] Bouabdallah, S. (2007). Design and control of quad-rotors with application to autonomous flying, Doctoral dissertation, Ecole Polytechnique Federale de Lausanne. p95-p105
- [14] Kawakami, Kiyobumi, et al. "The effect of sounds on newborn infants under stress." *Infant Behavior and Development*, 1996, 19(3): 375-379.
- [15] Iancu, Ion. A Mamdani type fuzzy logic controller. INTECH Open Access Publisher, 2012
- [16] Mizumoto, Masaharu, and Hans-Jürgen Zimmermann. "Comparison of fuzzy reasoning methods." *Fuzzy sets and systems*, 1982, 8(3): 253-283.
- [17] Wijayasekara, Dumidu, and Milos Manic. "Fuzzy logic based force-feedback for obstacle collision avoidance of robot manipulators. 2014 7th IEEE International Conference on Human System Interactions (HSI), page 76 – 81
- [1] <http://www.un.org/en/globalissues/demining/>